Low-Frequency Waves Generated by HF Heating of Mid-Latitude Ionosphere

A. Surjalal Sharma[1], Bengt Eliasson[1,2] , Xi Shao[1]
Gennady Mlikh[1] and Dennis Papadopoulos[1]

[1] Department of Astronomy, University of Maryland
College Park, Maryland 20742, USA

[2] SUPA, Physics Department, University of Strathclyde
Glasgow, Scotland G4 0NG, UK

ABSTRACT

High frequency (HF) heating of the ionsosphere excites hydromagnetic waves which propagate to the ground and into the magnetosphere. In the mid-latitude ionosphere, modulated HF heating in the F-region produces a local fluctuating electron temperature, and the resulting pressure gradient leads to a diamagnetic current which excites magnetosonic waves. In the E-region, where the Hall conductivity is dominant, these waves lead to oscillating Hall currents that produce shear Alfvén waves. The excitation of hydromagnetic waves in the mid-latitude ionosphere is simulated using Hall MHD model and taking into account the Earth's dipole magnetic field. With the heating in a region located at $L = 1.6$, altitude of 500 km and HF waves modulated at 2 – 10 Hz, the waves are generated by processes similar to the high-latitude case. The shear Alfven waves propagating to the magnetosphere become electromagnetic ion cyclotron waves at higher altitudes and propagate to the ion cyclotron resonance layer.

1. INTRODUCTION

Ionospheric heating experiments have enabled exploration of the ionosphere as a large-scale natural laboratory for the study of many plasma processes. These experiments inject high frequency (HF) radio waves into the overhead plasma using high power transmitters and an array of ground- and space-based diagnostics are used detect the ionospheric response. The modulated heating of the plasma lead to fluctuations in the ionospheric current system and associated controlled generation of low frequency waves [*Papadopoulos et al.,* 1989; 2011a, b; *Stubbe,* 1996]. The HF heating experiments conducted using the HAARP facility has generated low frequency waves [*Papadopoulos et al.,* 2011a, b] in all the three ranges, viz. ultra low frequency (ULF, <10 Hz), extremely low-frequency (ELF, 0.01 - 3 kHz) and very low frequency (VLF, 3-30 kHz).

The low frequency waves are generated in the ionosphere during heating experiments with modulated HF waves (1 – 10 MHz) due to multiple physical mechanisms which operate at different altitudes and conditions. One such mechanism is the modulation of the D/E-region conductivity by modulated HF heating and requires the presence of an electrojet current, viz. the auroral electrojet. The associated modification of the electrojet current creates an effective antenna radiating at the modulation frequency [*Papadopoulos et al.*, 1989; *Stubbe*, 1996]. This mechanism of low frequency wave generation by a modulated heating of the auroral electrojet, at ~ 80 km altitude in the D/E region, is referred to as the Polar Electrojet (PEJ) antenna. In another mechanism modulated HF waves heat the plasma in the F-region, producing a local hot spot and

thus a region of strong gradient in the plasma pressure. This leads to a diamagnetic current, on the time scale of the modulation frequency, and excites hydromagnetic waves, primarily in the magnetosonic branch. In this case there is no quasi-steady or background current and the wave excitation is controlled by the plasma conditions, HF modulation frequency, size of the heated region, etc. This mechanism has been studied in simulations of the high latitude ionosphere [*Papadopoulos et al.*, 2011a; *Eliasson et al.,* 2012] for conditions typically corresponding to the HAARP facility. Another mechanism for the generation of ELF waves was motivated by observations by the DEMETER satellite during experiments at HAARP with no modulation of the HF power. These waves have been identified as whistlers with frequencies consistent with lower hybrid waves generated by parametric processes [*Vartanyan et al.,* 2015].

The mid-latitude ionosphere has no steady large scale current or electrojet and modulated HF heating can generate low frequency waves due to the processes similar to the case of high-latitude ionosphere. Numerical simulations of the modulated heating in the mid-latitude ionosphere show that the geometry of Earth's dipole field plays an important role in their propagation to the magnetosphere. The modelling of excitation and propagation of low frequency waves in HF heating of the mid-latitude ionosphere are presented in this paper.

2. MODELING LOW-FREQUENCY WAVES IN HF HEATING

The hydromagnetic waves in the ionosphere are described in general by the MHD model, in which all plasma species are magnetized. The plasma density in the ionosphere has a maximum, with the corresponding Alfvén speed minimum, at an altitude of ~300 km. In the E-region altitudes of 80-120 km where the ion – neutral collision frequency v_{in} is larger than the ion cyclotron frequency ω_{ci}, the ions are strongly coupled to the neutrals, and the Hall conductivity dominates the dynamics. The dominant low frequency mode is the helicon mode [*Papadopoulos et al.,* 1994], which is the low frequency ($\omega << \omega_{ci}$) branch of whistler wave, and is carried by the electrons. In this region the Hall conductivity σ_H dominates over the Pedersen conductivity σ_P. This altitude dependence of the conductivities has important consequences in the propagation of waves, viz. mode conversion between magnetosonic and shear Alfven waves [*Hughes,* 1983].

The propagation of low frequency waves ($\omega << \omega_{ci} << \omega_{ce}$) in the ionosphere is described by a collisional Hall-MHD model of the plasma [*Eliasson et al.,* 2012]. Neglecting the electron inertia, the momentum equation governing the electron flow velocity $\mathbf{v_e}$ in the electric filed $\mathbf{E}$ and magnetic fields $\mathbf{B}$ becomes

$$0 = -\frac{e}{m_e}(\mathbf{E} - \mathbf{v}_e \times \mathbf{B}_0) - v_{en}\mathbf{v}_e - \frac{\nabla P_e}{n_0} \tag{1}$$

where $P_e(\mathbf{r}, t) = n_0 T_e(\mathbf{r}, t)$ is the modulated electron pressure due to local heating, *n* the electron density, $T_e(\mathbf{r}, t)$ the electron temperature in energy units, $v_{en}(\mathbf{r})$ the electron-neutral collision frequency, *e* the magnitude of the electron charge, and m_e the electron mass. The ion fluid velocity $\mathbf{v}_i$ is governed by the ion momentum equation

$$\frac{\partial \mathbf{v}_i}{\partial t} = \frac{e}{m_i}(\mathbf{E} - \mathbf{v}_i \times \mathbf{B}_0) - v_{in}\mathbf{v}_i \,, \tag{2}$$

where ν_{in} is the ion-neutral collision frequency and m_i is the ion mass. The electric and magnetic fields are governed by Faraday's and Ampère's laws:

$$\nabla \times \mathbf{E} = -\frac{\partial \mathbf{B}}{\partial t} \tag{3}$$

and

$$\nabla \times \mathbf{B} = \mu_0 e n_0(\mathbf{r})(\mathbf{v}_i - \mathbf{v}_e) \tag{4}$$

On the scales relevant to the low frequency waves the various processes due to the HF waves result in a local region with enhanced temperature and whose size and duration are determined by the beam size and modulation frequency, respectively. The processes at such the short scales do not play a direct role in this study and a volume averaged model in which the heated region with an enhanced electron pressure P_e. is used. In the numerical model, the electron temperature is assumed to have a Gaussian profile and with azimuthal symmetry:

$$T_e = T_{mod}\tanh^2\left(\frac{t}{D_t}\right)\cos(\omega t)\exp\left[-\frac{r_\theta^2}{L_r^2} - \frac{(z-z_o)^2}{L_z^2}\right], \tag{5}$$

where T_{mod} is the modulation amplitude of the electron temperature, D_t is the rise time, L_r is the width in the plane at $z = z_o$, L_z is the vertical width of the heated region and the heating is modulated at frequency ω. Similar to *Eliasson et al.* [2012], the slow mean temperature increase due to the HF heating is neglected as it will not contribute significantly to the wave-dynamics. For the study of wave excitation and propagation the plasma conductivity tensors obtained from the linearized equations are used. The conductivity along the magnetic field $\sigma_\parallel$ is determined by the electron and ion mobilities, and the high parallel conductivity serves to short circuit the parallel electric field. The Hall conductivity σ_H dominates over the Pedersen conductivity σ_P in the D and E regions, and the reverse is the case at higher altitudes.

The mid-latitude ionosphere has features, such as the curvature of Earth's dipole magnetic field and the absence of a steady current system, may lead to physical processes different from the high-latitude case. Simulations of the mid-latitude region thus require a model that takes these into account. A generalized model is derived from Eqs. (1) - (4) [*Eliasson et al.* 2012]:

$$\frac{\partial \mathbf{A}}{\partial t} = -\mathbf{E} \tag{6}$$

and

$$\frac{\partial \mathbf{E}}{\partial t} = -\omega_{ci}(\Gamma_{in} + \Gamma_{en})\mathbf{E} + \frac{\bar{\bar{\varepsilon}}^{-1}[\nabla \times (\nabla \times \mathbf{A})]}{\mu_0} - \frac{\bar{\bar{\mathbf{R}}}_e\,[\nabla \times (\nabla \times \mathbf{E})]}{\mu_0\tilde{\sigma}} + \left(\omega_{ci}\bar{\bar{\mathbf{R}}}_i - \frac{\partial}{\partial t}\right)\frac{\nabla P_e}{en_0} \tag{7}$$

where we introduced the vector and scalar potentials $\mathbf{A}$ and ϕ via $\mathbf{B} = \nabla \times \mathbf{A}$ and $\mathbf{E} = -\nabla\phi - \partial\mathbf{A}/\partial t$, using the gauge $\phi = 0$. The $\bar{\bar{\mathbf{R}}}_e$ and $\bar{\bar{\mathbf{R}}}_i$ matrices (organizing the vectors as column vectors) are deduced from the electron and ion equations of motion, viz. Eqs. (1) and (2), using the definitions $(\mathbf{v}_e \times \mathbf{B}_0 + m_e\nu_{en}\mathbf{v}_e/e)/B_0 \equiv \bar{\bar{\mathbf{R}}}_e\mathbf{v}_e$ and $(\mathbf{v}_i \times \mathbf{B}_0 - m_i\nu_{in}\mathbf{v}_i/e)/B_0 \equiv \bar{\bar{\mathbf{R}}}_i\mathbf{v}_i$, respectively. In doing so, the Cartesian coordinate system (x, y, z) of *Eliasson et al.* (1012) is here replaced by a spherical coordinate system (R, φ, θ) where R, φ and θ is the radial,

longitudinal and co-latitudinal coordinate, respectively. In the spherical coordinates, the magnitude of the dipole magnetic field is $B_0 = B_{eq}(R_E/R)^3\sqrt{1 + 3\cos^2\theta}$. The $\bar{\bar{\mathbf{R}}}_e$ and $\bar{\bar{\mathbf{R}}}_i$ matrices are used to construct the inverse of an effective dielectric tensor $\bar{\bar{\boldsymbol{\varepsilon}}}^{-1} = -(v_A^2/\varepsilon_0 c^2)\,\bar{\bar{\mathbf{R}}}_e\bar{\bar{\mathbf{R}}}_i$, where $v_A = c\omega_{ci}/\omega_{pi}$ is the Alfvén speed, and a conductivity tensor $\bar{\bar{\boldsymbol{\sigma}}} = \omega_{ci}(\Gamma_{in} + \Gamma_{en})\bar{\bar{\boldsymbol{\varepsilon}}}$, were we have denoted $\Gamma_{en} = v_{en}/\omega_{ce}$ and $\Gamma_{in} = v_{in}/\omega_{ci}$. Here, $\omega_{ci} = e\,B_0/m_i$ and $\omega_{ce} = e\,B_0/m_e$ are the ion and electron cyclotron frequencies, $\omega_{pi} = (n_0\,e^2/\varepsilon_0\,m_i)^{1/2}$ and $\omega_{pe} = (n_0 e^2/\varepsilon_0\,m_e)^{1/2}$ are the ion and electron plasma frequencies, $\varepsilon_0 = \mu_0/c^2$ is the electric permittivity in vacuum, c is the speed of light in vacuum, and $\tilde{\sigma} = \varepsilon_0\omega_{pe}^2/\omega_{ce}$.

The mid-latitude ionosphere has similar plasma profiles as the auroral region but the magnetic field geometry is significantly different in at least two ways. As shown in Figure 1, the field lines are oblique and curved, and can lead to changes in the propagation characteristics of the waves. Further, a wave front propagating out of a heated region in the mid-latitude ionosphere will intercept a wider area in the E-region where the shear Alfvén waves are excited.
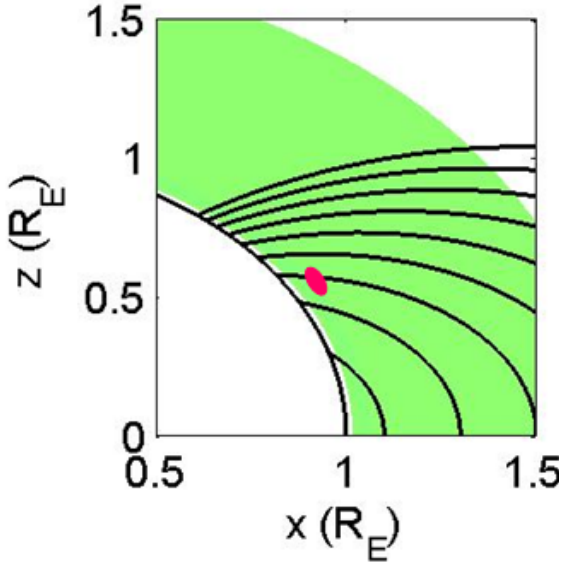

Figure 1. Part of the simulation domain (shaded in green) using polar coordinates in the mid-latitude region with the Earth's dipole magnetic field. The heated region (in red) is centered at the magnetic field line $L = 1.6$ [*Sharma et al.*, 2015a].

The simulations are conducted in a domain in the north-south plane in the spherical coordinates covering $R = R_E + 100$ km to $R_E + 4000$ km in the radial direction and a region $90°$ wide angular region in the co-latitudinal direction centered at the foot of the $L = 1.6$ shell, i.e. $\arcsin(1/\sqrt{L}) - 45° \le \theta \le \arcsin(1/\sqrt{L}) + 45°$. The simulation runs up to 12 seconds using 4×10^5 timesteps. The ionosphere is represented by a Chapman profile, with a peak density of 5×10^{10} m^{-3} at about 500 km, corresponding to a minimum of the Alfvén speed of $v_A \approx 900$ km/s. The simulation domain was resolved with 500 cells in the radial direction and 460 cells in the co-latitudinal direction. A centered 2nd-order difference scheme was used in the radial direction and a pseudo-spectral method with periodic boundary conditions in the co-latitudinal direction. The simulations were stopped before the waves reached the simulation boundaries in the co-latitudinal direction, hence eliminating the effects of the artificial periodic boundary conditions. First order outflow boundary conditions were used at the top boundary in the radial direction. At the lower boundary between the plasma and free space at $R = R_E + 100$ km, we have constructed boundary conditions, by assuming that the horizontal components of the electric field and vector potential, and their radial derivatives, are continuous. In free space, we have assumed infinite speed of light and that there are no electric charges or currents, while the ground at $R = R_E$ is perfectly conducting, so that

analytic approximations for the free space electromagnetic fields can be used (see *Eliasson et al.* 2012). In this setup T_e given by Eq. (5) peaks in the center of the heated region on the L shell. In these simulations $R_E = 6000$ km, $T_{mod} = 2000$ K, $D_t = 0.5$ s, $D_{r\theta} = 40$ km, $D_h = 20$ km, and $h_{max} = 300$ km, and $L = 1.6$.

The propagation of the low frequency waves into the magnetosphere, where the magnetic field is significantly reduced, leads to the possibility of their coupling to other modes, notably the electromagnetic ion cyclotron mode. For perpendicular propagation the compressional or magnetosonic waves ($\omega \simeq kv_A$) are excited. For parallel propagation and large wavenumbers $k \gtrsim c/\omega_{pi}$, the shear Alfvén mode splits into two modes, viz. the right-hand circularly polarized (R-mode) whistler and the left-hand circularly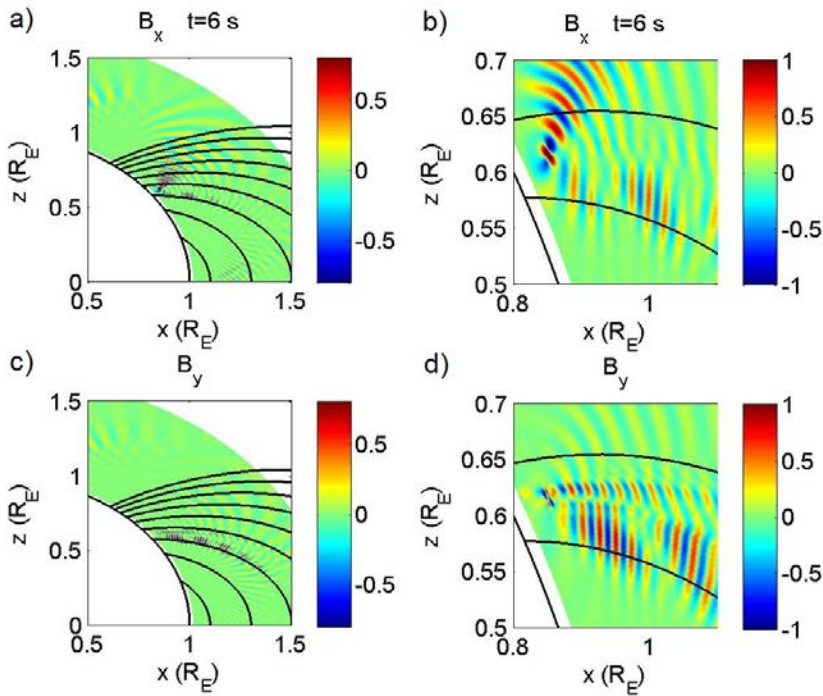 polarized (L-Mode) electromagnetic ion cyclotron (EMIC) mode, also known as the Alfvén-ion cyclotron mode. While the whistler mode can propagate at frequencies $\omega > \omega_{ci}$ at large wavenumbers, the EMIC propagates at frequencies $\omega < \omega_{ci}$ and has a resonance at ω_{ci} for large wavenumbers.

The excitation of both magnetosonic and shear Alfvén waves in the case of modulation at 5 Hz is shown in Figure 2. At frequencies much below the ion cyclotron frequency the shear Alfvén wave propagates primarily along the magnetic field lines. Magnetosonic waves (B_x) are created by the fluctuating diamagnetic current and propagate at large angles to the

Figure 2. Wave magnetic field (pT) of 5 Hz ELF waves excited by modulate ionospheric heating. The B_x component [panels a) and b)] is associated with magnetosonic waves, while the B_y component [panels c) and d)] is associated with shear Alfvén waves. Panels b) and d) show a close-up of a) and c), respectively, in the heated region [*Sharma et al.,* 2015a].

geomagnetic field lines upwards to the magnetosphere and downwards to E-region (Figure 2). Somewhat below the $L = 1.6$ magnetic field line extending from the heated region are whistler mode waves (cf. Figure 2d). These waves are not created in heated region but at the Hall region at the bottom of the ionosphere where magnetosonic waves have been mode converted to helicon waves, which propagate to higher altitudes as whistler waves. Near the heated region there is also a direct generation of EMIC waves.

5

As the wave frequency becomes comparable to the ion cyclotron frequency, the splitting of the shear Alfvén wave into the whistler and EMIC branches become more pronounced. The whistler wave is characterized by a longer wavelength and higher propagation speed than the EMIC wave at a given frequency. An interesting question is what happens when the EMIC reaches the ion cyclotron resonance at high altitudes, indicated by thin lines in Figures 2a and 2c. The simulations show that the10 Hz EMIC waves cannot propagate beyond ion cyclotron resonance layer where their wavelength goes to zero, and the EMIC wave energy will pile up near the resonance [*Sharma et al*., 2015a, b].

The HF heating experiments in the mid-latitude ionosphere using the facilities at Arecibo [*Ganguly et al.,* 1986], Platteville [*Utlaut et al.,* 1974] and Sura [*Kotik et al*., 2013] have provided a range of observations. The Arecibo experiment used transmitters at 3.1 and 5.1 MHz and the detectors were located 7 and 150 km offsite. In one experiment the HF frequencies were offset by predetermined frequencies in the ULF range, and the power spectra of the waves detected on the ground showed peaks at these frequencies. The detected ULF waves were interpreted as resulting from nonlinear coupling between the two transmitted waves. In another experiment the HF wave was modulated at ULF frequencies and there was a good coincidence between the HF wave transmission and the detection of ULF at the modulation frequency. The Plattevile experiments used transmitters with 5- 10- MHz in a ring array and detected the formation of field aligned artificial irregularities in the ionograms but there was no direct evidence of excited waves [*Utlaut et al.,* 1974]. The experiment using the Sura facility (4.5 – 9 MHz, three ground detectors 2.6, 9.5 and 13.7 km offsite in a nearly linear array) provided the first comprehensive evidence of the generation of hydromagnetic waves by modulated heating of the mid-latitude ionosphere [*Kotik et al*., 2013]. The effects of many factors, e. g., the wave polarization, geomagnetic activity and dependence on HF power, were examined in many experiments. The observations were interpreted as due to the HF waves heating the plasma due to nonlinear coupling [*Gurevich,* 1978] in a ring shaped region and the resulting pressure gradient leading to a ponderomotive force that is responsible for the low frequency wave excitation.

3. CONCLUSIONS

The generation of low frequency hydromagnetic waves is a main feature of HF heating of the ionosphere. The nunerical simulations and experiments using HAARP facility have yielded a comprehensive understanding of the plasma processes in the ionosphere that leads to wave generation. In the high-latitude ionosphere these waves are excited under most conditions, viz. with or without an auroral electrojet. The essential mechanism is a multi-step process in which the pressure gradient in the heated region in the F region drives a local diamagnetic current, which excites magnetosonic waves propagating across the magnetic field and in turn excites shear Alfvén waves in the E region. The dominance of the Hall conductivity over the Pederson conductivity due to the strong coupling of the ion and nutral dynamics is responsible for the conversion of the compressional to shear modes. The propagation of the shear Alfvén waves along the field lines, to the ground and to the magnetosphere, have been detected by ground and satellite based measurements.

In the mid-latitude ionosphere where there is no steady current or electrojet, the hydromagnetic waves are generated by essentially the same mechanism. The simulations for this case take into

account the curved geometry of the Earth's dipole field and show new features in the generation of EMIC waves in the magnetosphere. In the equatorial ionosphere where the equatorial electrojet is prevalent, HF heating is expected to generate low frequency waves by the same mechanism as in the high- and mid-latitudes. A striking feature of the equatorial ionosphere is its highly enhanced Cowling conductivity, which can lead to more efficient wave generation [*Eliasson and Papadopoulos,* 2009; *Jain et al*., 2012]. The Cowling conductivity, which is associated with the equatorial electrojet, can be larger than the conductivity associated with the auroral elctrojet by two orders of magnitude, and thus can potentially magnify the wave generation significantly.

The hydromagnetic waves in the ionosphere and magnetosphere play key roles in a variety of processes and have been observed by ground-based detectors and low-earth orbit satellites. The numerical simulations, such as these presented here, identify the plasma processes underlying the observations and thus provide a comprehensive understanding.

REFERENCES
Eliasson, B., & Papadopoulos, K., (2009). Penetration of ELF Currents and Electromagnetic Fields into Earth's Equatorial Ionosphere, J. Geophys. Res., 114, A10301.

Eliasson, B., Chang, C.-L., & Papadopoulos, K. (2012). Generation of ELF and ULF electromagnetic waves by modulated heating of the ionospheric F2 region, J. Geophys. Res., 117, doi:10.1029/2012JA017935.

Ganguly, S., Gordon, W., & Papadopoulos, K. (1986). Active Nonlinear Ultralow-frequency Generation in the Ionosphere, *Phys. Rev. Lett., 57*, 641-644, doi:10.1103/PhysRevLett.57.641.

Gurevich, A. V. (1978). *Nonlinear Phenomena in the Ionosphere*, Springer, New York.

Jain, N., Eliasson, B., Sharma, A. S., & Papadopoulos, K (2012). Penetration of ELF Currents and Electromagnetic Fields into the Off-equatorial E-region of the Earth's Ionosphere, arXiv:1201.5349v1 [physics.plasm-ph].

Hughes, W. J. (1983). Hydromagnetic waves in the magnetosphere, Rev. Geophys. Space Phys., 21, 508-520.

Kotik D.S., Ryabov, A. V., Ermakova, E. N., Pershin, A. V., Ivanov, V. N., & Esin, V. P. (2013). Properties of ULF / VLF signals generated by SURA facility in the upper ionosphere, Radiophys. and Quant. Electr. 56(6), 344-354.

Papadopoulos, K., Sharma, A. S., & Chang, C. L. (1989). On the Efficient Operation of a Plasma ELF Antenna Driven by Modulation of Ionospheric Currents, Comm. Plasma Phys. and Cont. Fus., 13(1), 1-17.

Papadopoulos, K., Zhou, H.-B., & Sharma, A. S. (1994). The Role of Helicon Waves in Magnetospheric and Ionospheric Physics, Comm. Plasma Phys. & Cont. Fusion, 15(6), 321-337..

Papadopoulos, K., Gumerov, N., Shao, X., Chang, C. L., & Doxas, I. (2011a). HF driven currents in the ionosphere, *Geophys. Res. Lett., 38,* L12103, doi:10.1029/2011GL047368.

Papadopoulos, K., Chang, C.-L., Labenski, J. & Wallace, T. (2011b). First Demonstration of HF-driven Ionospheric Currents, Geophys. Res. Lett., 38, L20107, doi:10.1029/2011GL049263.

Sharma, A. S., B. Eliasson, X. Shao and K. Papadopoulos (2015a). Excitation of low frequency waves in HF heating in the mid-latitude ionosphere, *J. Geophys. Res.,* to be submitted.

Sharma, A. S., B. Eliasson, X. Shao and K. Papadopoulos (2015b). Low Frequency Waves in HF Heating of the Ionosphere, in *Low Frequency Waves in Space Plasmas,* eds. A. Keiling, D.-H. Lee, K.-H. Glassmeier and V. Nakariakov, Amer. Geophys. Union, Washington, DC., in press.

Stubbe, P., (1996). Review of Ionospheric Modification Experiments at Tromso, *J. Atmos. Terr. Phys., 58*, 349-368.

Vartanyan, A., Milikh, G. M., Eliasson, B., Najmi, A. C., Chang, C. L., Parrot, M., & Papadopoulos, K. (2015). Generation of Whistler Waves by Continuous HF Heating of the Upper Ionosphere. Geophys. Res. Lett., submitted.

Utlaut, W. F., Viollette, E. J., & Melanson, L. L. (1974). Radar Cross-section Measurements and Vertical Incidence Effects Observed with Platteville at Reduced Power, Radio Sci., 9(11), 1033-1040, doi:10.1029/RS009i011p01033.